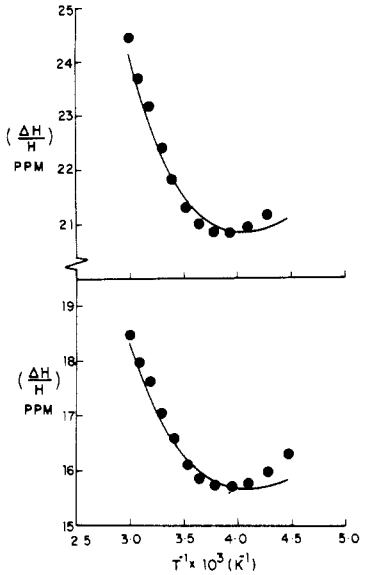


**Figure 10.** Temperature dependence of the experimental and theoretical IPS for two sets of "low-spin" methyl resonances of hemin chloride in pyridine–chloroform solution. The circles are the experimental data. The solid lines are the theoretically calculated ones for $\Delta = 950$ cm$^{-1}$ and ln $C = 2$. The hyperfine coupling constants (MHz) for the upper theoretical curve are $A(^2T_{2g}) = 0.60$ and $A(^6A_1) = 0.63$, while for the lower curve $A(^2T_{2g}) = 0.45$ and $A(^6A_1) = 0.49$.

($\zeta$) are included. Figure 9 shows a series of test calculations with varying $\Delta$ (the energy separation between $^6A_1$ and $^2T_2$) and ln $C$, $\zeta$ and $A_i$ being held constant. The results bring out the sensitive nature of these parameters to the IPS and the close similarity of the theoretical plots to the experimental data of Figure 7. From these plots, the parameter-space region of possible fits to the experimental data was delineated, which helped in obtaining the best fit to the experimentally observed temperature dependence of the methyl IPS. A result of such a fit is shown in Figure 10. The fit is good, and the values of the parameters appear reasonable. These values of parameters may not be unique since a similar fit may be obtained by a slightly different choice of $\Delta$, ln $C$, and the $A_i$ values. However, as evident from Figure 9, the range of the values of these parameters for acceptable fits to the experimental data is very narrow, and hence the present set of parameters define closely their true values. The significant point is the observation that the $S = {}^5/_2 \rightleftharpoons S = {}^1/_2$ thermal spin-equilibrium model reproduces closely the unusual temperature dependence of the IPS of the methyl protons of these complexes. It seems therefore certain that the bis(pyridine)hemin chloride complexes in pyridine–chloroform solution are not pure "low-spin" but are involved in the spin equilibrium between high- and low-spin states. The same holds true for Fe(DPDMe)Cl in the pyridine–chloroform solution as well. The present study does not however support the previous suggestion of $S = {}^3/_2 \rightleftharpoons S = {}^1/_2$ spin equilibrium.

## Conclusion

The present proton magnetic resonance study shows that hemin chloride in pure pyridine contains both high- and low-spin iron(III) porphyrin complexes that are in exchange with each other. The high-spin iron(III) complex is believed to be a six-coordinated (pyridine)hemin chloride, which has one pyridine and one chloride ligand axial to the ferric ion. This is rather an uncommon stereochemistry for the iron porphyrin. The low-spin complex is the bis(pyridine)iron(III) porphyrin, in which two pyridine molecules are axially coordinated to the iron. This is a common structural form that has several analogues in the heme chemistry.[33] The addition of chloroform to this solution has a marked effect especially in very small quantities. The proton NMR spectra of Figure 6 seem to suggest a chemical equilibrium between the mono(pyridine) and the bis(pyridine) complexes since the peaks of the two complexes move toward each other as chloroform is added in small amounts.[36] The bis(pyridine)iron(III) porphyrin complex in the pyridine–chloroform solution is stereochemically the same complex as in the pure pyridine solution, but while in the pyridine–chloroform solution it shows a thermal spin equilibrium between $S = {}^5/_2$ and $S = {}^1/_2$, it behaves almost as low spin in the pure pyridine solution. Evidently the dilution of the pyridine solution with chloroform causes the subtle difference that changes the electronic structure of the bis(pyridine)ferric porphyrin complexes. Finally, it is observed that in pyridine solution the iron(III) porphyrin is slowly reduced to the iron(II) porphyrin, while in pyridine–chloroform solution this reduction is considerably less.

**Acknowledgment.** The NMR studies were carried out at the 500-MHz FT NMR National Facility, which is gratefully acknowledged. O.K.M. thanks Gauhati University for a leave of absence.

(36) The spectra in Figure 6 seem to provide evidence of rapid equilibrium between the high- and low-spin bis(pyridine) complexes since the peaks of the two species move toward each other as chloroform is added in small amounts. According to a reviewer, the reason for the increased rate of ligand exchange when chloroform is added could have something to do with hydrogen bonding from chloroform to the chloride ion, which could both encourage breaking the Fe–Cl bond of the mono(pyridine) complex and also help solvate the chloride ion of the bis(pyridine) complex.

Contribution from the Department of Chemistry, The University of North Carolina, Chapel Hill, North Carolina 27514

# Electrocatalytic Reduction of Nitrite to Nitrous Oxide and Ammonia Based on the N-Methylated, Cationic Iron Porphyrin Complex $[Fe^{III}(H_2O)(TMPyP)]^{5+}$

Mark H. Barley, Matthew R. Rhodes, and Thomas J. Meyer*

*Received July 11, 1986*

An electrochemical study of the N-methylated, cationic iron porphyrin complex $[Fe^{III}(H_2O)(TMPyP)]^{5+}$ (TMPyP = *meso*-tetrakis(*N*-methyl-4-pyridyl)porphine dication) has shown that the complex is an effective electrocatalyst for the reduction of nitrite to $N_2O$, $NH_3$, and, by inference, hydroxylamine at a potential of −0.65 V (vs. SCE); reduction at −0.9 V leads to a decrease in the relative amount of $N_2O$ produced.

## Introduction

The reduction of nitrite to ammonia involves a six-electron–seven-proton change as shown in eq 1. In biological systems the

$$NO_2^- + 8H^+ + 6e^- \rightarrow NH_4^+ + 2H_2O \qquad (1)$$

$$E^\circ \text{ (vs. SCE at pH 7)} = +0.103 \text{ V}$$

net reaction is catalyzed by the nitrite reductase enzymes in which the active site is based on the iron–heme prosthetic group.[1] Although in a net sense the nitrite/ammonia interconversion is a complex reaction, relatively simple metal complexes have been

(1) Losada, M. *J. Mol. Catal.* **1975**, *1*, 245.

0020-1669/87/1326-1746$01.50/0 

identified in which both oxidation of coordinated ammonia to nitrosyl and reduction of coordinated nitrosyl to ammonia occur.[2,3] Electrochemical studies on polypyridyl complexes of osmium and ruthenium have revealed that the first stage in the interconversion between bound nitrite and ammonia is a simple acid–base reaction in which a bound nitro group is converted into nitrosyl, eq 2.

$$[(bpy)_2(py)Ru\text{–}NO_2]^+ + 2H^+ \rightarrow [(bpy)_2(py)Ru\text{–}NO]^{3+} + H_2O \quad (2)$$

Conversion to the nitrosyl form has, at the same time, the effect of removing one of the oxide anions from the nitrogen center and creating low-lying $\pi^*$-based levels at the NO group,[4] which, in turn, provide the basis for a series of ligand-based reductions. Although polypyridyl complexes of ruthenium and osmium are not electrocatalysts for the interconversions of nitrite and ammonia because of strong ligand binding, it was recently reported that the water-soluble, anionic iron porpyrhin complex $[Fe^{III}(H_2O)(TPPS)]^{3-}$ (TPPS is the *meso*-tetrakis(4-sulfonatophenyl)porphine sexianion) is an effective catalyst and that at least the initial steps involved parallel those observed for complexes of ruthenium and osmium.[5,6] In addition, a series of complexes of iron have been reported to act as electrocatalysts for the reduction of NO,[7] and detailed spectroscopic and electrochemical studies on the reduction of iron porphyrin nitrosyls in nonaqueous solvents have appeared.[8,9]

Here we report the results of a series of studies on the electrocatalyzed reduction of nitrite by the cationic, pyridinium-based porphine $[(Fe^{III}(H_2O)(TMPyP)]^{5+}$ (TMPyP is *meso*-tetrakis(*N*-methyl-4-pyridyl)porphine dication).[10] The structure of the macrocyclic ring system is shown below. Our interests in the cationic porphine system were to establish the generality of the iron porphine based electrocatalyzed reduction of nitrite in aqueous solution, to explore the possible effects of the peripheral pyridinium groups as electron reservoirs or electrostatic sites, and to explore the role of the electrolysis potential in determining the product distribution.

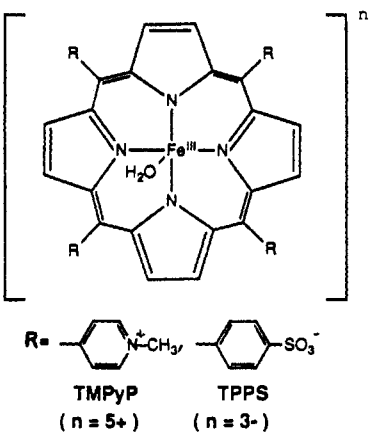


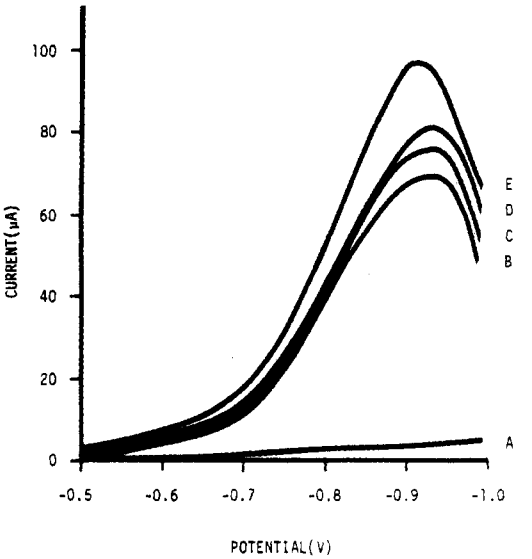


**Figure 1.** Linear-sweep voltammograms on solutions containing $NaNO_2$ in 0.1 M acetic acid (pH 2.87) in the presence and absence of $[Fe^{III}(H_2O)(TMPyP)]^{5+}$. Conditions: scan rate = 100 mV/s; 0.28-$cm^2$ glassy-carbon electrode; potentials vs. SCE; $[NO_2^-]$ = 0.01 M and [Fe] = 0, $3.5 \times 10^{-6}$, $7.0 \times 10^{-6}$, and $14.0 \times 10^{-6}$ M for curves A–D, respectively; $[NO_2^-]$ = 0.015 M and [Fe] = $14.0 \times 10^{-6}$ M for curve E. Under these conditions the concentration of catalyst is sufficiently low that its intrinsic redox processes do not contribute significantly to the background.

## Experimental Section

**Electrochemistry.** The instrumentation, cells and materials used here have been described in detail elsewhere.[5] Unless indicated otherwise the electrodes used in the voltammetric experiments were 0.28-$cm^2$ glassy-carbon electrodes and all potentials are vs. the saturated calomel electrode (SCE).

**Preparation of $[Fe^{III}(H_2O)(TMPyP)]_2(SO_4)_5$.** Preparation of the iron porphyrin complex was based on the method of Pasternack et al.[10] A 83-mg sample of $[H_2(TMPyP)](SO_4)_2$ produced by anion exchange of $[H_2(TMPyP)]I_4$ (Strem) was heated at reflux for 2–4 h in water with 10 equiv of $FeSO_4$ (or ferrous ammonium sulfate). The pH was checked periodically and corrected to between 4 and 5 with 0.1 M NaOH. The reaction was stopped when spectral studies indicated the absence of unmetalated porphine. The most sensitive test for the presence of free-base porphine was found to be the presence of strong absorption bands at 430, 490, and 704 nm due to protonated forms of the porphine, e.g. $[H_4(TMPyP)]^{6+}$ in strongly acidic media such as 0.1 M $H_2SO_4$.

Once the metalation reaction was complete the solution was filtered, an excess of concentrated $NaClO_4$ solution was added to the filtrate, and the resulting solution was stirred overnight to coarsen the precipitate. The insoluble salt $[Fe^{III}(H_2O)(TMPyP)](ClO_4)_5$ was collected by using a centrifuge yielding 170 mg of product. *Caution should be observed in handling this compound as it has been reported to be explosive,*[11] *although no problems were encountered in handling it in this laboratory.* The solid was placed in an anion exchange column (Dowex 1X8-50, Aldrich) in the sulfate form and eluted with sulfuric acid (0.1 M) to give a solution of $[Fe^{III}(H_2O)(TMPyP)]^{5+}$ and $SO_4^{2-}$. The resulting solution was rotovapped to a brown solid and dried under vacuum to give the salt $[Fe^{III}(H_2O)(TMPyP)]_2(SO_4)_5$. The product was hygroscopic and was stored in a desiccator.

Molar extinction coefficients (in $M^{-1}$ $cm^{-1}$) were estimated for the complex by measuring the absorbances of solutions containing the complex with a Bausch & Lomb Spectronic 2000 spectrometer. The complex was subsequently precipitated quantitatively as the perchlorate salt and weighed to determine the concentration in the solution. The peaks observed correspond well to those previously reported under similar conditions.[12] UV/vis data: at pH 0.9 (0.1 M $H_2SO_4$), $\lambda_{max}$ (log $\epsilon$) = 408 (5.06 (Soret, broad), 512 (4.21), and 632 nm (3.85); at pH 2.87 (0.1 M acetic acid), $\lambda_{max}$(log $\epsilon$) = 414 (5.05) (Soret, broad), 502 (4.23), and 630 nm (3.90).

(2) (a) Thompson, M. S.; Meyer, T. J. *J. Am. Chem. Soc.* **1981**, *103*, 5577. (b) Murphy, R. W., Jr.; Takeuchi, K. J.; Barley, M. H.; Meyer, T. J. *Inorg. Chem.* **1986**, *25*, 1041. (c) Murphy, W. R., Jr.; Takeuchi, K. J.; Meyer, T. J. *J. Am. Chem. Soc.* **1982**, *104*, 5817.
(3) (a) Bottomley, F.; Mukaida, M. *J. Chem. Soc., Dalton Trans.* **1982**, 1933. (b) Armor, J. *Inorg. Chem.* **1973**, *12*, 1959.
(4) (a) Bottomley, F. J. *J. Chem. Soc., Dalton Trans.* **1974**, 1600. (b) Ennemark, J. H.; Feltham, R. D. *Coord. Chem. Rev.* **1974**, *13*, 339. (c) Bottomley, F. *Coord. Chem. Rev.* **1978**, *26*, 7. (d) Pipes, D. W.; Meyer, T. J. *Inorg. Chem.* **1984**, *23*, 2466.
(5) Barley, M. H.; Takeuchi, K. J.; Meyer, T. J. *J. Am. Chem. Soc.* **1986**, *108*, 5876.
(6) Barley, M. H.; Takeuchi, K. J.; Murphy, W. R., Jr.; Meyer, T. J. *J. Chem. Soc., Chem. Commun.* **1985**, 507.
(7) (a) Uchiyana, S.; Muto, G. *J. Electroanal. Chem. Interfacial Electrochem.* **1981**, *127*, 275. (b) Ogwa, K.; Ishikawa, H. *J. Chem. Soc., Faraday Trans. 1* **1984**, *80*, 2243.
(8) Olson, L. W.; Schaeper, D.; Lancon, D.; Kadish, K. M. *J. Am. Chem. Soc.* **1982**, *104*, 2042.
(9) Lancon, D.; Kadish, K. M. *J. Am. Chem. Soc.* **1983**, *105*, 5610.
(10) Pasternack, R. F.; Lee, H.; Malek, P.; Spencer, C. *J. Inorg. Nucl. Chem.* **1977**, *39*, 1865.
(11) Kurihara, H.; Arifuku, F.; Ando, I.; Saita, M.; Nishino, R.; Ujimoto, K. *Inorg. Chem.* **1982**, *55*, 3515.
(12) Harris, F. L.; Topper, D. L. *Inorg. Chem.* **1978**, *17*, 71.

## Results and Discussion

From earlier work, the solution chemistry of $[Fe^{III}(H_2O)(TMPyP)]^{5+}$ is reasonably well-defined. Under alkaline conditions a green $\mu$-oxo dimer is formed as reported previously[11-13] and as observed for other water-soluble iron porphyrin complexes.[14,15] However, the complex is monomeric as $Fe^{III}$ to pH ~5. It is also known that loss of the first proton from water bound to the $Fe^{III}$ and $Fe^{II}$ forms of the complex occurs above pH 5.[11,13] All of our electrochemical measurements were carried out in acidic solutions where the proton and solution compositions are well-defined.

**Evidence for Catalysis.** Cyclic voltammograms of $NaNO_2$ at pH 2.87 show a current enhancement in the presence of $[Fe^{III}(H_2O)(TMPyP)]_2(SO_4)_{10}$ that is not observed in the absence of the complex (Figure 1). A current response of 3.5 $\mu$A at −0.9 V (vs. SCE) is observed at a 0.28-cm$^2$ glassy-carbon electrode in the absence of the complex with $[NO_2^-]$ = 0.01 M (Figure 1A). Upon addition of the $Fe^{III}$ salt, a large catalytic wave develops at potentials more negative than −0.6 V and catalytic currents as high as 70 $\mu$A are observed at −0.9 V (Figure 1B–D) even when the concentration of complex is sufficiently low, $(3.5–14) \times 10^{-6}$ M, that it does not contribute to the background even though reduction at the pyridinium-based groups of the porphine occur in this potential region (see below). The catalytic current response is dependent on the amount of added $NO_2^-$ as evidenced by the increase in current observed upon addition of more nitrite to the solutions (Figure 1E). The current–potential profile of the catalytic manifold is featureless except for a wave that appears at $E_p \sim -0.9$ V at pH 2.87 shown in Figure 1. Although we have not studied the quantitative dependence of the catalytic current on either the complex or $NO_2^-$ concentrations, it is apparent from the data in Figure 1 that the catalyzed process depends upon both in the concentration ranges cited.

**Electrochemistry of $[Fe^{III}(H_2O)(TMPyP)]_2(SO_4)_5$.** A cyclic voltammogram of $[Fe^{III}(H_2O)(TMPyP)]_2(SO_4)_5$ in 0.1 M $H_2SO_4$ (Figure 2A) displays a quasi-reversible reduction at $E_{p,c} = -0.18$ V; $E_{p,a} = -0.01$ V at a scan rate of 100 mV/s arising from the $[Fe(H_2O)(TMPyP)]^{5+/4+}$ ($Fe^{III/II}$) couple. When the scan rate was reduced to 20 mV/s the peak-to-peak splitting is reduced to $\Delta E_p$ = 150 mV with $E_{1/2} = -0.11$ V, which agrees well with values obtained earlier.[11,13]

In addition to the metal-centered reduction, a multielectron wave is observed at potentials more negative than −0.7 V. In differential-pulse polarograms (inset, Figure 2A) a $[Fe(H_2O)(TMPyP)]^{5+/4+}$ reduction wave appears as a well-defined peak at −0.1 V and the multielectron wave appears at −0.81 V. The multielectron wave is due to the reduction of the peripheral *N*-methylpyridinium groups on the porphine.

**Electrochemistry of $[Fe^{III}(H_2O)(TMPyP)]^{5+}$ in the Presence of Nitrite.** Addition of 10 equiv of $NO_2^-$ to a solution of $10^{-3}$ M in porphine complex and 0.1 M in $H_2SO_4$ causes the metal-centered reduction wave at −0.11 V to disappear from the voltammograms, and a new, broad catalytic wave to appear at $E_p \sim -0.6$ V, which distorts the 4-electron pyridinium-based wave at −0.8 V (Figure 2B).

A cyclic voltammogram of a solution containing the porphine complex in 0.1 M acetic acid (pH 2.87) containing a 1:1 nitrite to porphine ratio at an oxidatively activated carbon electrode[16] shows a broad cathodic wave for the $Fe^{III} \rightarrow Fe^{II}$ reduction of the $[Fe(H_2O)(TMPyP)]^{5+/4+}$ couple at −0.23 V. The current increases rapidly at potentials past −0.5 V due both to the catalyst reduction of nitrite and to the multielectron pyridinium-based reduction at −0.8 V (Figure 3A). Under these conditions an addition reduction wave is observed as a shoulder at $E_{p,c} = -0.6$ V with a distinctive return component at $E_{p,a} = -0.45$ V. In addition, a wave appears at +0.55 V just before the onset of the wave for the oxidation of free nitrite. The wave at +0.55 V probably arises from the

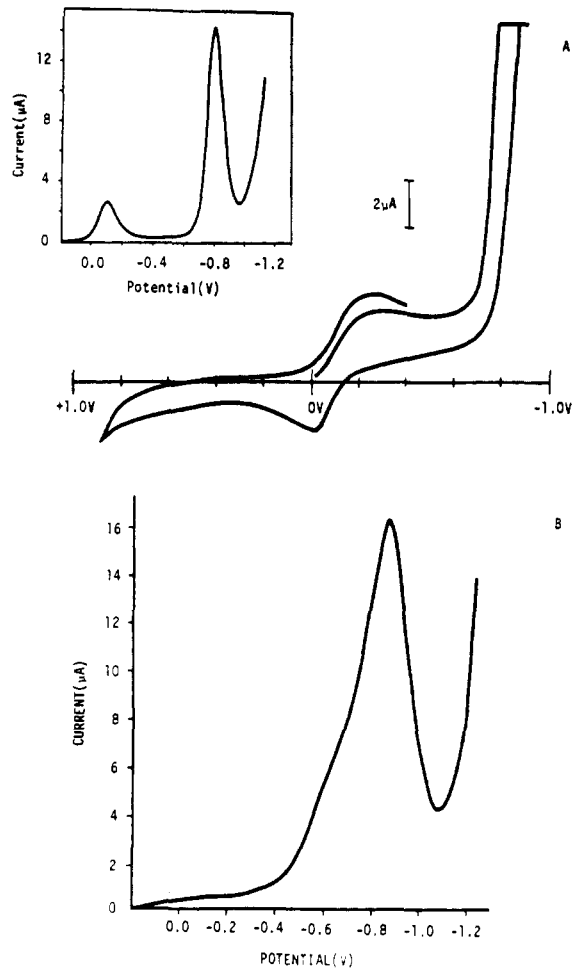


**Figure 2.** (A) Cyclic voltammogram with a differential-pulse polarogram shown as an inset of 1 mM $[Fe^{III}(H_2O)(TMPyP)]_2(SO_4)_5$ in 0.1 M $H_2SO_4$. Conditions: CV scan rate = 100 mV/s; DPP scan rate = 10 mV/s; potentials vs. SCE at a glassy-carbon electrode of 0.28-cm$^2$ area. (B) Differential-pulse polarogram of 0.7 mM $[Fe^{III}(H_2O)(TMPyP)]_2(SO_4)_5$ in 0.1 M $H_2SO_4$ with 10 equiv of $NO_2^-$ added per Fe(III) porphine. Scan rate = 10 mV/s.

$Fe^{II}(NO^+)/Fe^{II}(NO^\bullet)$ couple $[Fe^{II}(NO)(TMPyP)]^{5+/4+}$ by analogy to the $[Fe^{II}(NO)(TPPS)]^{3-/4-}$ couple, which is observed at $E_{p,a}$ = +0.35 V (pH 3.01).[5] The wave at $E_{1/2} = -0.52$ V is analogous to a wave observed at $E_{1/2} = -0.63$ V (pH 3.01) for the $Fe^{II}(NO^\bullet)/Fe^{II}(NO^-)$ couple[5] $[Fe^{II}(NO)(TPPS)]^{4-/5-}$ and probably arises from the corresponding $[Fe^{II}(NO)(TMPyP)]^{4+/3+}$ nitrosyl-based reduction. After sweeping reductively to −0.9 V, the usually well-defined $[Fe(H_2O)(TMPyP)]^{5+/4+}$ oxidation at $E_{p,a} \simeq 0.0$ V is completely missing on the return oxidative scan. By inference, reduction of bound NO past the 2-electron-reduction stage occurs in the catalytic envelope in Figure 3 to give $N_2O$, $NH_2OH$, and/or $NH_3$, as noted below, which is rapid on the CV time scale. During the short time required for the return scan, the reduced N-based product is lost from an axial coordination site and the nitrosyl complex re-forms.

Differential-pulse polarograms of solutions containing 1 equiv of added $NO_2^-$ at pH 2.87 (Figure 3B) still show a residual peak for the $[Fe(H_2O)(TMPyP)]^{5+/4+}$ couple at −0.08 V. However, following reduction to $Fe^{II}$, the NO complex rapidly forms as shown by the appearance of a distinct peak at −0.57 V for the $[Fe^{II}(NO)(TMPyP)]^{5+/4+}$ couple. The NO-based reduction is followed by the pyridinium-based multielectron reduction at ~−0.8 V. A complication that appears after a period of several minutes is that the amount of nitrosyl complex formed upon reduction decreases because of a loss of nitrite from the solution via[5]

$$3HONO \rightarrow NO_3^- + 2NO + H_2O + H^+$$

The available electrochemical evidence shows that in qualitative

(13) Forshey, P. A.; Kuwana, T. *Inorg. Chem.* **1981**, *20*, 693.
(14) Peterson, M. W.; Richman, R. M. *Inorg. Chem.* **1985**, *24*, 722.
(15) Thompson, A. M.; Krishnamurthy, M. *Inorg. Chim. Acta* **1979**, *34*, 145.
(16) Cabaniss, G. E.; Diamantis, A. A.; Murphy, W. R., Jr.; Linton, R. W.; Meyer, T. J. *J. Am. Chem. Soc.* **1985**, *107*, 1845.

**Table I.** Products of Electrocatalytic Reductions at $E_{app}$ = −0.65 V vs. SCE[a]

| run | [Fe], M | $[NO_2^-]$, M | $[NO_2^-]$/[Fe] | pH | time, h | current, μA $i_i$ | current, μA $i_f$ | tot. charge, C | current efficiency,[b] % $N_2O$ | current efficiency,[b] % $NH_3$ | current efficiency,[b] % $NH_2OH$ | product distribn,[c] % $N_2O$ | product distribn,[c] % $NH_3$ | product distribn,[c] % $NH_2OH$ | product distribn,[c] % $NO_2^-$ |
|---|---|---|---|---|---|---|---|---|---|---|---|---|---|---|---|
| 1 | $7.5 \times 10^{-3}$ | 0.02 | 280 | 6.7 | 44 | 2.8 | 0.15 | 232.4 | 33 | 67 | 0 | 54 | 36 | 0 | 15 |
| 2 | $3.43 \times 10^{-4}$ | 0.01 | 29 | 4.5 | 6 | 18.0 | 2.5 | 144.7 | 22 | 78 | 0 | 45 | 55 | 0 | 0 |
| 3 | $1.9 \times 10^{-4}$ | 0.02 | 100 | 4.5 | 14 | 27.0 | 0.07 | 231.8 | 37 | 55 | 8 | 63 | 30 | 7 | 0 |

[a] All electrolyses were carried to completion except for run 1 (90% complete) so that turnover numbers for the catalyst on a per nitrite basis are the same as the ratio of nitrite to iron porphine complex. Current densities can be calculated by dividing the currents listed by the area of the mercury pool electrode (4.91 $cm^2$). [b] Current efficiency is given as moles of product formed multiplied by the $n$ value for its formation (e.g. $n$ = 2 for $N_2O$; $n$ = 6 for $NH_3$) divided by the total charge passed during the experiment. The moles of $N_2O$ and $NH_3$ were calculated from GC assays. The amount of charge transferred from the initial reduction of $Fe^{III}$ to $Fe^{II}$ is negligible in comparison to the total charge passed. [c] Product distributions were determined by GC analysis of the solution in the cell and the atmosphere above it at the end of the experiment. The amount of $NO_2^-$ listed for the first run assumed that since no charge was unaccounted for, the balance of nitrogen missing was due to unreduced nitrite. The amount of $NH_2OH$ listed in run 3 is calculated on the basis of the otherwise unaccounted for charge passed and initial nitrite added and was not directly determined. Difficulties in the direct analysis of $NH_2OH$ were discussed previously.[5]

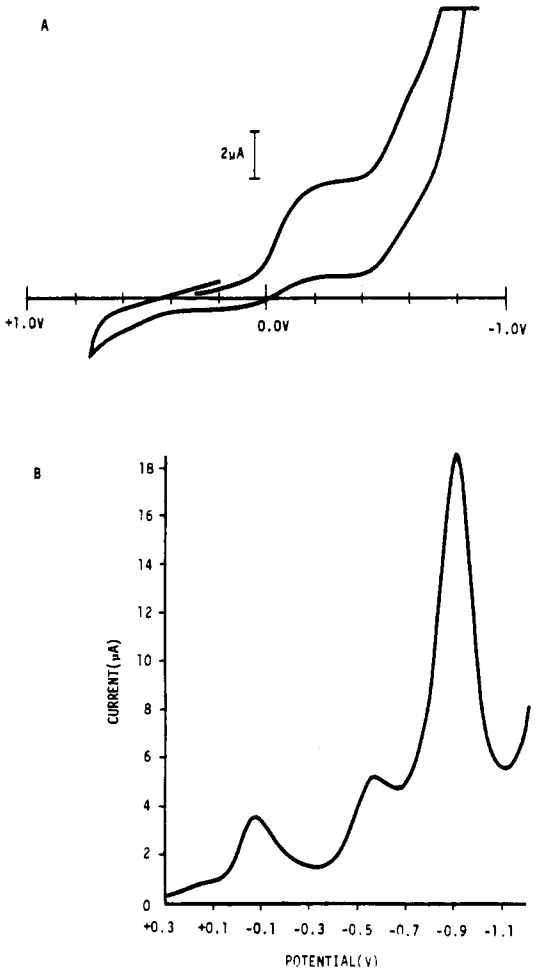


**Figure 3.** (A) Cyclic voltammogram of a solution containing $[Fe^{III}(H_2O)(TMPyP)]_2(SO_4)_5$ and 1 equiv of added $NO_2^-$ per Fe(III) porphine (1 mM) in 0.1 M acetic acid with a scan rate of 100 mV/s. (b) Differential-pulse polarogram of the same solution at a scan rate of 10 mV/s. Unless otherwise given, conditions are as in Figure 2.

detail, the electrochemical properties of acidic solutions containing either $[Fe^{III}(H_2O)(TPPS)]^{3-}$ or $[Fe^{III}(H_2O)(TMPyP)]^{5+}$ with added nitrite are very similar. Initial reduction of $Fe^{III}$ to $Fe^{II}$ results in the rapid formation of a nitrosyl complex via

$$[Fe^{II}(H_2O)(TMPyP)]^{4+} + 2H^+ + NO_2^- \rightarrow [Fe^{II}(NO^+)(TMPyP)]^{5+} + H_2O \quad (3)$$

The nitrosyl complex undergoes successive 1-electron reductions

$$[Fe^{II}(NO^+)(TMPyP)]^{5+} + e^- \rightarrow [Fe^{II}(NO^\bullet)(TMPyP)]^{4+} \quad E^{\circ\prime} = +0.55 \text{ V}$$

$$[Fe^{II}(NO^\bullet)(TMPyP)]^{4+} + e^- \rightarrow [Fe(NO)(TMPyP)]^{3+} \quad E^{\circ\prime} = -0.57 \text{ V}$$

at potentials (vs. SCE) that are comparable to those observed for the analogous TPPS complex. Following the second reduction, a further multiple-electron process occurs for both porphine complexes in the same potential range and is rapid as shown by the reappearance of $[Fe^{II}(NO^\bullet)(TMPyP)]^{4+}$ or $[Fe^{II}(NO)(TPPS)]^{4-}$ on the reverse, oxidative scan. Although the same pattern of redox events occurs for the two systems, a question remains as to the possible influence of electrostatic effects on the product distribution and, more importantly, of the possible "electron reservoir" effect of the reduction pyridinium groups in the TMPyP complex. The net reduction of $NO_2^-$ to $NH_2OH$ or $NH_3$ are multielectron in character, and past the 2-electron stage

$$[Fe^{II}(NO^+)(TMPyP)]^{5+} \xrightarrow{+2e^-} [Fe(NO)(TMPyP)]^{3+}$$

there is a further 4-electron requirement to reach $NH_3$, which, at least in principle, could be assisted kinetically by electrons initially stored at the pyridinium sites on the ring.

**Bulk Electrocatalytic Experiments.** The results of three bulk electrocatalytic reductions are summarized in Table I. The reductions were carried out at $E_{app}$ = −0.65 V to avoid contributions from the pyridinium-based reduction at −0.8 V. At −0.65 V and pH 7, a relatively slow electrolysis occurred that eventually gave >90% conversion of nitrite to ammonia and nitrous oxide as determined by gas chromatography (Table I). No assay was made for $N_2$, and if present as a reduction product, it must be a trace component given the current efficiencies for $N_2O$ and $NH_3$, which are clearly the major products. Under these conditions hydroxylamine appears to be only a very minor product, however, it may be a significant intermediate that upon formation undergoes further reduction as observed earlier for $NO_2^-$ reduction by $[Fe^{II}(H_2O)(TPPS)]^{4-}$ at pH 4.5.[5]

Reduction at −0.9 V with pH 4.5 gave a product distribution similar to that reported earlier when $[Fe^{III}(H_2O)(TPPS)]^{3-}$ was used as the electrocatalyst under similar conditions.[5] At this potential the production of $N_2O$ is considerably diminished (~21% for the TMPyP complex and ~18% for the TPPS complex), $NH_3$ remains a significant product (~35% and ~45%, respectively), and hydroxylamine formation also becomes significant (~44% vs. ~37%). Given the similarity in product distribution between the two porphine systems at pH 4.5, there is no obvious reason to ascribe any special feature to the 4-electron-reservoir character of the reduction at the pyridinium groups at least in terms of product selectivity. In fact, the Fe–NO-based reduction chemistry past the $n$ = 2 stage appears to be similar for the anionic and cationic porphines as suggested by the appearance of the catalytic wave for nitrite reduction in the same potential region for each. However, the question of relative rates remains open, and it is conceivable that initial reduction at the pyridinium sites followed by intramolecular electron transfer to the catalytically active Fe–NO site does lead to a considerable rate advantage.

From observations made during the catalytic runs at $E_{app}$ = −0.9 V, competitive, irreversible reduction of the tetramethylpyridinium sites does not appear to be a problem until the electrolysis of nitrite is nearly complete. After complete reduction of nitrite, the solution becomes pale yellow and then intense green

**Scheme I**

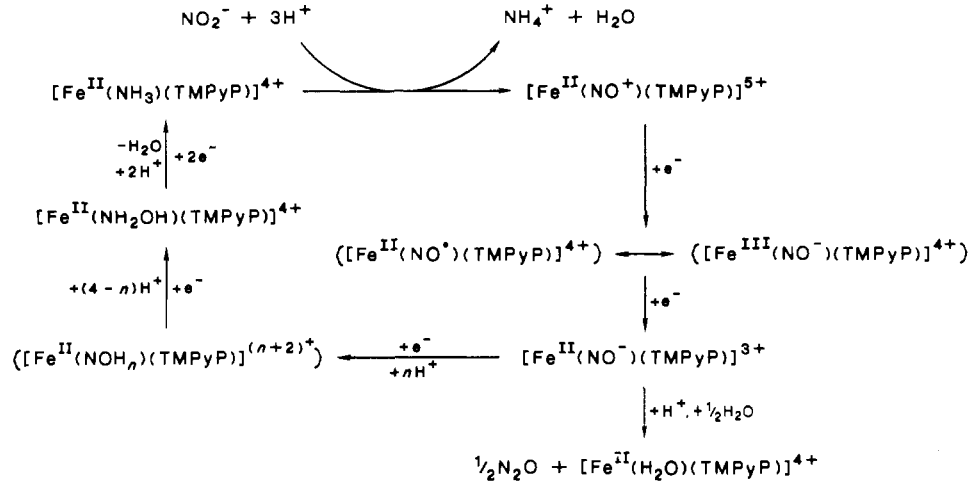


upon aerial oxidation, suggesting that in water at pH 4.5 irreversible reduction of the pyridinium sites does occur.

Reduction potentials (vs. SCE) for $NO_2^-$ to the various reduced products observed in the electrolyses at pH 7 are given below. For all cases the net electrochemical reductions[17]

$$6H^+ + 2NO_2^- + 4e^- \rightarrow N_2O + 3H_2O \quad E^\circ = +0.527 \text{ V}$$

$$8H^+ + 2NO_2^- + 6e^- \rightarrow N_2 + 4H_2O \quad E^\circ = +0.723 \text{ V}$$

$$5H^+ + NO_2^- + 4e^- \rightarrow NH_2OH + H_2O \quad E^\circ = -0.190 \text{ V}$$

$$8H^+ + NO_2^- + 6e^- \rightarrow NH_4^+ + 2H_2O \quad E^\circ = +0.103 \text{ V}$$

(vs. SCE at pH 7) are highly spontaneous for $E_{app} = -0.65$ or $-0.90$ V, and although the reactions are catalyzed by the iron porphine complexes, there is a high overvoltage in all cases. There is no obvious correlation between driving force and the observed product distribution, and in order to account for the appearance of the various products, it is necessary to consider the probable mechanism of reduction.

**Reduction Mechanism.** The results of the cyclic voltammetry and differential-pulse polarography experiments, which provide evidence for two initial 1-electron reductions, combined with inferences from the bulk electrolysis results and the earlier results obtained for the $[Fe^{III}(H_2O)(TPPS)]^{3-}$ system provides the basis for the overall reduction mechanism given in Scheme I. The scheme also shares certain steps in common with the stepwise redox interconversion of $M^{II}(NO^+)$ to $M^{II}(NH_3)$ in polypyridyl complexes of Ru and Os.[2] Intermediates for which there is no evidence or for which there are alternate formulations are shown by the use of braces. Following the reduction of $Fe^{III}$ to $Fe^{II}$, nitrosyl formation, and the two nitrosyl-based reductions, a multielectron catalytic step occurs that rapidly leads to the reduced products and returns the system to the nitrosyl form. $N_2O$ is the expected N–N coupling product at the 2-electron stage, presumably via eq 4. N–N coupling to give $N_2O$ must be in competition with

$$H_2O + 2[Fe^{II}(NO^-)(TMPyP)]^{3+} + 2H^+ \rightarrow 2[Fe^{II}(H_2O)(TMPyP)]^{4+} + N_2O \quad (4)$$

further reduction at the electrode, which is consistent with the effect of $E_{app}$ on the relative amount of $N_2O$ formed. At $E_{app} = -0.65$ V and pH 7, the electrode potential is past $E_p$ for the second reduction and on the rising portion of the wave for the multielectron step. At $E_{app} = -0.9$ V, the potential is past the peak of the multielectron wave and the rate of reductive capture of the 2-electron-reduced intermediate is enhanced relative to N–N coupling.

The absence of any significant N–N coupling to give $N_2$ suggests that if a subsequent 1-electron intermediate builds up in the solution at the 3-electron stages, as has been observed for polypyridyl complexes of Os and Ru,[2b,c] it may be as the hydrate, e.g., $[Fe^{II}(NH_2O)(TMPyP)]^{4+}$, rather than as the nitrido form, $[Fe^{V}(N)(TMPyP)]^{4+}$, since the nitrido form might be expected to undergo rapid coupling to give $N_2$. Subsequent reduction of the 3-electron intermediate to the $NH_2OH$ stage presumably occurs, probably releasing $NH_2OH$ to the solution, with $NH_2OH$ undergoing further electrocatalytic reduction as has been observed for $[Fe^{III}(H_2O)(TPPS)]^{3-}$.[5] Further mechanistic insight into the 2-electron-induced coupling and production of $N_2O$ is currently under investigation based on polyprydiyl complexes of Ru and Os.

**Acknowledgments** are made to the National Institutes of Health under Grant No. 5-R01-GM32296-03 for support of this research.

(17) Latimer, W. M. *Oxidation Potentials*, 2nd ed.; Prentice-Hall: Englewood Cliffs, NJ, 1952; pp 90, 95, 97, and 104.